ScienceDirect

Journal of Trace Elements in Medicine and Biology

Volume 46, March 2018, Pages 76-82

Aluminium in brain tissue in autism

Matthew Mold [a], Dorcas Umar [b], Andrew King [c], Christopher Exley [a]

Show more

https://doi.org/10.1016/j.jtemb.2017.11.012

Get rights and content

Under a Creative Commons license

open access

Abstract

Autism spectrum disorder is a neurodevelopmental disorder of unknown aetiology. It is suggested to involve both genetic susceptibility and environmental factors including in the latter environmental toxins. Human exposure to the environmental toxin aluminium has been linked, if tentatively, to autism spectrum disorder. Herein we have used transversely heated graphite furnace atomic absorption spectrometry to measure, for the first time, the aluminium content of brain tissue from donors with a diagnosis of autism. We have also used an aluminium-selective fluor to identify aluminium in brain tissue using fluorescence microscopy. The aluminium content of brain tissue in autism was consistently high. The mean (standard deviation) aluminium content across all 5 individuals for each lobe were 3.82(5.42), 2.30(2.00), 2.79(4.05) and 3.82(5.17) μg/g dry wt. for the occipital, frontal, temporal and parietal lobes respectively. These are some of the highest values for aluminium in human brain tissue yet recorded and one has to question why, for example, the aluminium content of the occipital lobe of a 15 year old boy would be 8.74 (11.59) μg/g dry wt.? Aluminium-selective fluorescence microscopy was used to identify aluminium in brain tissue in 10 donors. While aluminium was imaged associated with neurones it appeared to be present intracellularly in microglia-like cells and other inflammatory non-neuronal cells in the meninges, vasculature, grey and white matter. The pre-eminence of intracellular aluminium associated with non-neuronal cells was a standout observation in autism brain tissue and may offer clues as to both the origin of the brain aluminium as well as a putative role in autism spectrum disorder.

Previous article

Next article

Keywords

Human exposure to aluminium; Human brain tissue; Autism spectrum disorder; Transversely heated atomic absorption spectrometry; Aluminium-selective fluorescence microscopy

1. Introduction

Autism spectrum disorder (ASD) is a group of neurodevelopmental conditions of unknown cause. It is highly likely that both genetic [1] and environmental [2] factors are associated with the onset and progress of ASD while the mechanisms underlying its aetiology are expected to be multifactorial [3], [4], [5], [6]. Human exposure to aluminium has been implicated in ASD with conclusions being equivocal [7], [8], [9], [10]. To-date the majority of studies have used hair as their indicator of human exposure to aluminium while aluminium in blood and urine have also been used to a much more limited extent. Paediatric vaccines that include an aluminium adjuvant are an indirect measure of infant exposure to aluminium and their burgeoning use has been directly correlated with increasing prevalence of ASD [11]. Animal models of ASD continue to support a connection with aluminium and to aluminium adjuvants used in human vaccinations in particular [12]. Hitherto there are no previous reports of aluminium in brain tissue from donors who died with a diagnosis of ASD. We have measured aluminium in brain tissue in autism and identified the location of aluminium in these tissues.

2. Materials and methods

2.1. Measurement of aluminium in brain tissues

Ethical approval was obtained along with tissues from the Oxford Brain Bank (15/SC/0639). Samples of cortex of approximately 1 g frozen weight from temporal, frontal, parietal and occipital lobes and hippocampus (0.3 g only) were obtained from 5 individuals with ADI-R-confirmed (Autism Diagnostic Interview-Revised) ASD, 4 males and 1 female, aged 15–50 years old (Table 1).

Table 1. Aluminium content of occipital (O), frontal (F), temporal (T) and parietal (P) lobes and hippocampus (H) of brain tissue from 5 donors with a diagnosis of autism spectrum disorder.

Donor ID	Gender	Age	Lobe	Replicate	[Al] μg/g
A1	F	44	O	1	0.49
				2	4.26
				3	0.33
				Mean (SD)	1.69 (2.22)
			F	1	0.98
				2	1.10
				3	0.95
				Mean (SD)	1.01 (0.08)
			T	1	1.13
				2	1.16
				3	1.12
				Mean (SD)	1.14 (0.02)
			P	1	0.54
				2	1.18
				3	NA
				Mean (SD)	0.86 (0.45)
			All	Mean (SD)	1.20 (1.06)
A2	M	50	O	1	3.73
				2	7.87
				3	3.49
				Mean (SD)	5.03 (2.46)
			F	1	0.86
				2	0.88
				3	1.65
				Mean (SD)	1.13 (0.45)
			T	1	1.31
				2	1.02
				3	2.73
				Mean (SD)	1.69 (0.92)
			P	1	18.57
				2	0.01
				3	0.64
				Mean (SD)	6.41 (10.54)

			Hip.	1	1.42
			All	Mean (SD)	3.40 (5.00)
A3	M	22	O	1	0.64
				2	2.01
				3	0.66
				Mean (SD)	1.10 (0.79)
			F	1	1.72
				2	4.14
				3	2.73
				Mean (SD)	2.86 (1.22)
			T	1	1.62
				2	4.25
				3	2.57
				Mean (SD)	2.81 (1.33)
			P	1	0.13
				2	3.12
				3	5.18
				Mean (SD)	2.82 (1.81)
			All	Mean (SD)	2.40 (1.58)
A4	M	15	O	1	2.44
				2	1.66
				3	22.11
				Mean (SD)	8.74 (11.59)
			F	1	1.11
				2	3.23
				3	1.66
				Mean (SD)	2.00 (1.10)
			T	1	1.10
				2	1.83
				3	1.54
				Mean (SD)	1.49 (0.37)
			P	1	1.38
				2	6.71
				3	NA
				Mean (SD)	4.05 (3.77)
			Hip.	1	0.02
			All	Mean (SD)	3.73 (6.02)

A5	M	33	O	1	3.13
				2	2.78
				3	1.71
				Mean (SD)	2.54 (0.74)
			F	1	2.97
				2	8.27
				3	NA
				Mean (SD)	5.62 (3.75)
			T	1	1.71
				2	1.64
				3	17.10
				Mean (SD)	6.82 (8.91)
			P	1	5.53
				2	2.89
				3	NA
				Mean (SD)	4.21 (1.87)
			All	Mean (SD)	4.77 (4.79)

The aluminium content of these tissues was measured by an established and fully validated method [13] that herein is described only briefly. Thawed tissues were cut using a stainless steel blade to give individual samples of ca 0.3 g (3 sample replicates for each lobe except for hippocampus where the tissue was used as supplied) wet weight and dried to a constant weight at 37 °C. Dried and weighed tissues were digested in a microwave (MARS Xpress CEM Microwave Technology Ltd.) in a mixture of 1 mL 15.8 M HNO_3 (Fisher Analytical Grade) and 1 mL 30% w/v H_2O_2 (BDH Aristar). Digests were clear with no fatty residues and, upon cooling, were made up to 5 mL volume using ultrapure water (cond.<0.067 μS/cm). Total aluminium was measured in each sample by transversely heated graphite furnace atomic absorption spectrometry (TH GFAAS) using matrix-matched standards and an established analytical programme alongside previously validated quality assurance data [13].

2.2. Fluorescence microscopy

All chemicals were from Sigma Aldrich (UK) unless otherwise stated. Where available frontal, parietal, occipital, temporal and hippocampal tissue from 10 donors (3 females and 7 males) with a diagnosis of ASD was supplied by the Oxford Brain Bank as three 5 μm thick serial paraffin-embedded brain tissue sections per lobe for each donor (Table S1). Tissue sections mounted on glass slides were placed in a slide rack and de-waxed and rehydrated via transfer through 250 mL of the following reagents: 3 min in Histo-Clear (National Diagnostics, US), 1 min in fresh Histo-Clear, 2 min in 100% v/v ethanol (HPLC grade) and 1 min in 95, 70, 50 & 30% v/v ethanol followed by rehydration in ultrapure water (cond.<0.067 μS/cm) for 35 s. Slides were agitated every 20 s in each solvent and blotted on tissue paper between transfers to minimise solvent carry-over. Rehydrated brain tissue sections were carefully outlined with a PAP pen for staining, in order to form a hydrophobic barrier around the periphery of tissue sections. In between staining, tissue sections were kept hydrated with ultrapure water and stored in moisture chambers, to prevent sections from drying out. Staining was staggered to allow for accurate incubation times of brain tissue sections. We have developed and optimised the fluor lumogallion as a selective stain for aluminium in cells [14] and human tissues [15]. Lumogallion (4-chloro-3-(2,4-dihydroxyphenylazo)-2-hydroxybenzene-1-sulphonic acid, TCI Europe N.V. Belgium) was prepared at ca 1 mM via dilution in a 50 mM PIPES (1,4-Piperazinediethanesulphonic acid) buffer, adjusted to pH 7.4 with NaOH. Lumogallion staining was performed via the addition of 200 μL of the staining solution to rehydrated brain tissue sections that were subsequently incubated at ambient temperature away from light for 45 min. Sections for autofluorescence analyses were incubated for 45 min in 200 μL 50 mM PIPES buffer only, pH 7.4. Following staining, glass slides containing tissue sections were washed six times with 200 μL aliquots of 50 mM PIPES buffer, pH 7.4, prior to rinsing for 30 s in ultrapure water. Serial sections numbered 1 and 2 for each lobe were incubated in 50 mM PIPES buffer, pH 7.4 or stained with 1 mM lumogallion in the same buffer, respectively, to ensure consistency across donor tissues.

All tissue sections were subsequently mounted under glass coverslips using the aqueous mounting medium, Fluoromount™. Slides were stored horizontally for 24 h at 4 °C away from light, prior to analysis via fluorescence microscopy.

Stained and mounted human brain tissue sections were analysed via the use of an Olympus BX50 fluorescence microscope, equipped with a vertical illuminator and BX-FLA reflected light fluorescence attachment (mercury source). Micrographs were obtained at X 400 magnification by use of a X 40 Plan-Fluorite objective (Olympus, UK). Lumogallion-reactive aluminium and related autofluorescence micrographs were obtained via use of a U-MNIB3 fluorescence filter cube (excitation: 470–495 nm, dichromatic mirror: 505 nm, longpass emission: 510 nm, Olympus, UK). Light exposure and transmission values were fixed across respective staining treatment conditions and images were obtained using the CellD software suite (Olympus, Soft Imaging Solutions, SiS, GmbH). Lumogallion-reactive regions identified through sequential screening of stained human brain tissue sections were additionally imaged on autofluorescence serial sections, to assess the contribution of the fluorophore. The subsequent merging of fluorescence and bright-field channels was achieved using Photoshop (Adobe Systems Inc. US). When determining intracellular staining the type of cells stained were estimated by their size and shape in the context of the brain area sampled and their surrounding cellular environment.

3. Results

3.1. Aluminium content of brain tissues

The aluminium content of all tissues ranged from 0.01 (the limit of quantitation) to 22.11 μg/g dry wt. (Table 1). The aluminium content for whole brains (n = 4 or 5 depending upon the availability of hippocampus tissue) ranged from 1.20 (1.06) μg/g dry wt. for the 44 year old female donor (A1) to 4.77 (4.79) μg/g dry wt. for a 33 year old male donor (A5). Previous measurements of brain aluminium, including our 60 brain study [13], have allowed us to define loose categories of brain aluminium content beginning with ≤1.00 μg/g dry wt. as pathologically benign (as opposed to 'normal'). Approximately 40% of tissues (24/59) had an aluminium content considered as pathologically-concerning (≥2.00 μg/g dry wt.) while approximately 67% of these tissues had an aluminium content considered as pathologically-significant (≥3.00 μg/g dry wt.). The brains of all 5 individuals had at least one tissue with a pathologically-significant content of aluminium. The brains of 4 individuals had at least one tissue with an aluminium content ≥5.00 μg/g dry wt. while 3 of these had at least one tissue with an aluminium content ≥10.00 μg/g dry wt. (Table 1). The mean (SD) aluminium content across all 5 individuals for each lobe were 3.82(5.42), 2.30(2.00), 2.79(4.05) and 3.82(5.17) μg/g dry wt. for the occipital, frontal, temporal and parietal lobes respectively. There were no statistically significant differences in aluminium content between any of the 4 lobes.

3.2. Aluminium fluorescence in brain tissues

We examined serial brain sections from 10 individuals (3 females and 7 males) who died with a diagnosis of ASD and recorded the presence of aluminium in these tissues (Table S1). Excitation of the complex of aluminium and lumogallion emits characteristic orange fluorescence that appears increasingly bright yellow at higher fluorescence intensities. Aluminium, identified as lumogallion-reactive deposits, was recorded in at least one tissue in all 10 individuals. Autofluorescence of immediately adjacent serial sections confirmed lumogallion fluorescence as indicative of aluminium. Deposits of aluminium were significantly more prevalent in males (129 in 7 individuals) than females (21 in 3 individuals). Aluminium was found in both white (62 deposits) and grey (88 deposits) matter. In females the majority of aluminium deposits were identified as extracellular (15/21) whereas in males the opposite was the case with 80 out of 129 deposits being intracellular. We were only supplied with 3 serial sections of each tissue and so we were not able to do any staining for general morphology which meant that it was not always possible to determine which subtype of cell was showing aluminium fluorescence.

Aluminium-loaded mononuclear white blood cells, probably lymphocytes, were identified in the meninges and possibly in the process of entering brain tissue from the lymphatic system (Fig. 1). Aluminium could be clearly seen inside cells as either discrete punctate deposits or as bright yellow fluorescence. Aluminium was located in inflammatory cells associated with the vasculature (Fig. 2). In one case what looks like an aluminium-loaded lymphocyte or monocyte was noted within a blood vessel lumen surrounded by red blood cells while another probable lymphocyte showing intense yellow fluorescence was noted in the adventitia (Fig. 2b). Glial cells including microglia-like cells that showed positive aluminium fluorescence were often observed in brain tissue in the vicinity of aluminium-stained extracellular deposits (Fig. 3, Fig. 4). Discrete deposits of aluminium approximately 1 μm in diameter were clearly visible in both round and amoeboid glial cell bodies (e.g. Fig. 3b). Intracellular aluminium was identified in likely neurones and glia-like cells and often in the vicinity of or co-localised with lipofuscin (Fig. 5). Aluminium-selective fluorescence microscopy was successful in identifying aluminium in extracellular and intracellular locations in neurones and non-neuronal cells and across all brain tissues studied (Fig. 1, Fig. 2, Fig. 3, Fig. 4, Fig. 5). The method only identifies aluminium as evidenced by large areas of brain tissue without any characteristic aluminium-positive fluorescence (Fig. S1).

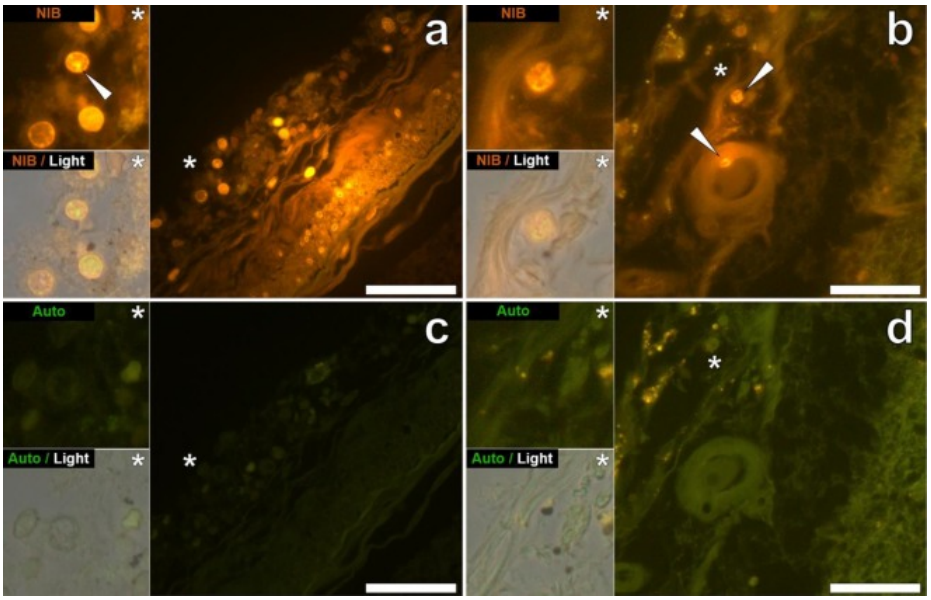

Download high-res image (634KB) Download full-size image

Fig. 1. Mononuclear inflammatory cells (probably lymphocytes) in leptomeningeal membranes in the hippocampus and frontal lobe of a 50-year-old male donor (A2), diagnosed with autism. Intracellular lumogallion-reactive aluminium was noted via punctate orange fluorescence emission (white arrows) in the hippocampus **(a)** and frontal lobe **(b)**. A green autofluorescence emission was detected in the adjacent non-stained (5 μm) serial section **(c & d)**. Upper and lower panels depict magnified inserts marked by asterisks, of the fluorescence channel and bright field overlay. Magnification ×400, scale bars: 50 μm. (For interpretation of the references to colour in this figure legend, the reader is referred to the web version of this article.)

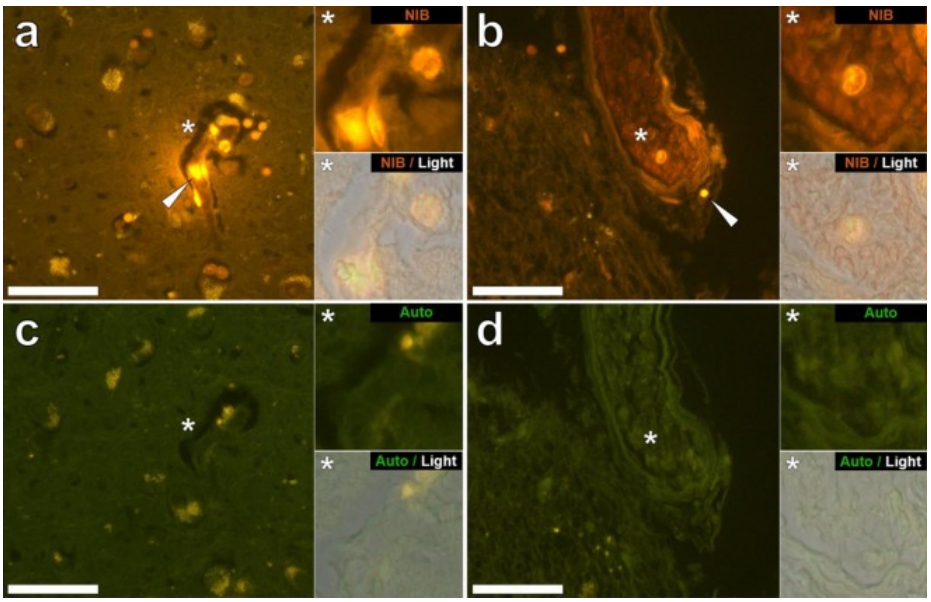

Download high-res image (700KB) Download full-size image

Fig. 2. Intracellular lumogallion-reactive aluminium in the vasculature of the hippocampus of a 50-year-old male donor (A2), diagnosed with autism. Aluminium-loaded inflammatory cells noted in the hippocampus in the vessel wall (white arrow) **(a)** and depicting punctate orange fluorescence in the lumen **(b)** are highlighted. An inflammatory cell in the vessel adventitia was also noted (white arrow) **(b)**. Lumogallion-reactive aluminium was identified via an orange fluorescence emission **(a & b)** versus a green autofluorescence emission **(c & d)** of the adjacent non-stained (5 μm) serial section. Upper and lower panels depict magnified inserts marked by asterisks, of the fluorescence channel and bright field overlay. Magnification ×400, scale bars: 50 μm. (For interpretation of the references to colour in this figure legend, the reader is referred to the web version of this article.)

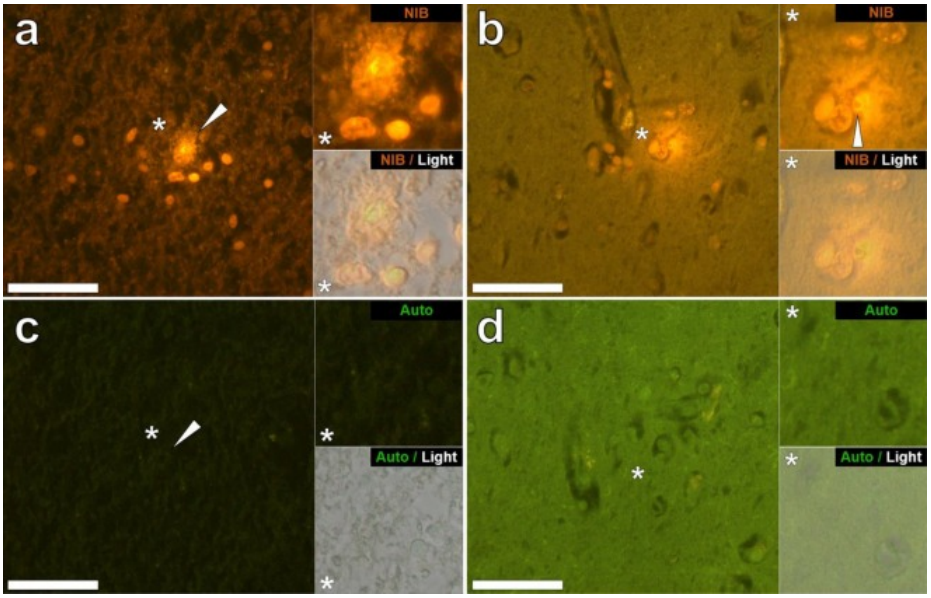

Download high-res image (743KB) Download full-size image

Fig. 3. Intracellular aluminium in cells morphologically compatible with glia and neurones in the hippocampus of a 15-year-old male donor (A4), diagnosed with autism. Lumogallion reactive cellular aluminium identified within glial-like cells in the hippocampus **(a)** and producing a punctate orange fluorescence in glia surrounding a likely neuronal cell within the parietal lobe **(b)** are highlighted (white arrows). Lumogallion-reactive aluminium was identified via an orange fluorescence emission **(a & b)** versus a green autofluorescence emission **(c & d)** of the subsequent non-stained (5 μm) serial section (white arrow/asterisk). Upper and lower panels depict magnified inserts marked by asterisks, of the fluorescence channel and bright field overlay. Magnification ×400, scale bars: 50 μm. (For interpretation of the references to colour in this figure legend, the reader is referred to the web version of this article.)

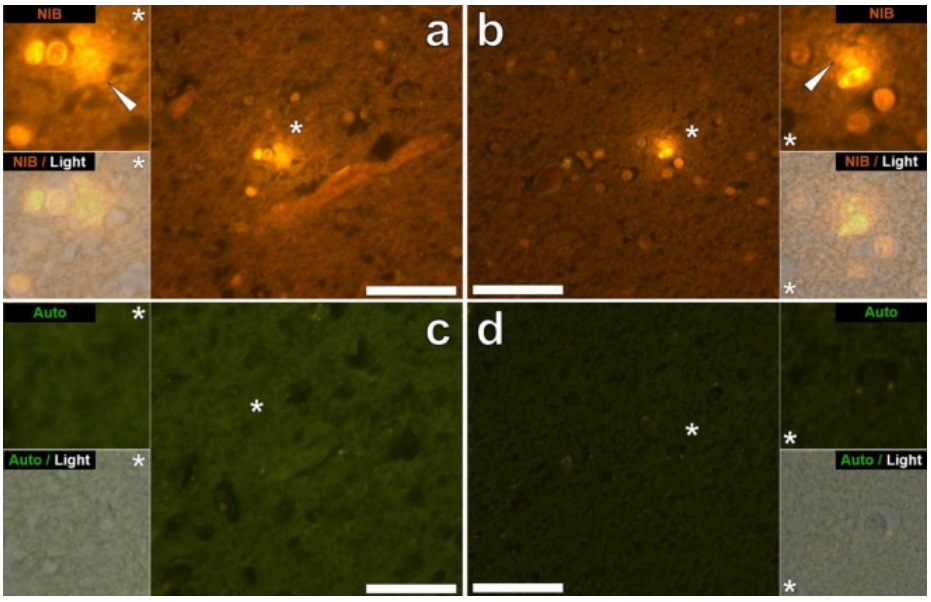

Download high-res image (694KB) Download full-size image

Fig. 4. Intracellular aluminium in cells morphologically compatible with microglia within the parietal and temporal lobes of 29-year-old (A8) and 15-year-old (A4) male donors, diagnosed with autism. Lumogallion-reactive extracellular aluminium (white arrows) producing an orange fluorescence emission was noted around likely microglial cells in the parietal **(a)** and temporal lobes **(b)** of donors A8 and A4 respectively. Non-stained adjacent (5 μm) serial sections, produced a weak green autofluorescence emission of the identical area imaged in white **(c)** and grey matter **(d)** of the respective lobes. Upper and lower panels depict magnified inserts marked by asterisks, of the fluorescence channel and bright field overlay. Magnification ×400, scale bars: 50 μm. (For interpretation of the references to colour in this figure legend, the reader is referred to the web version of this article.)

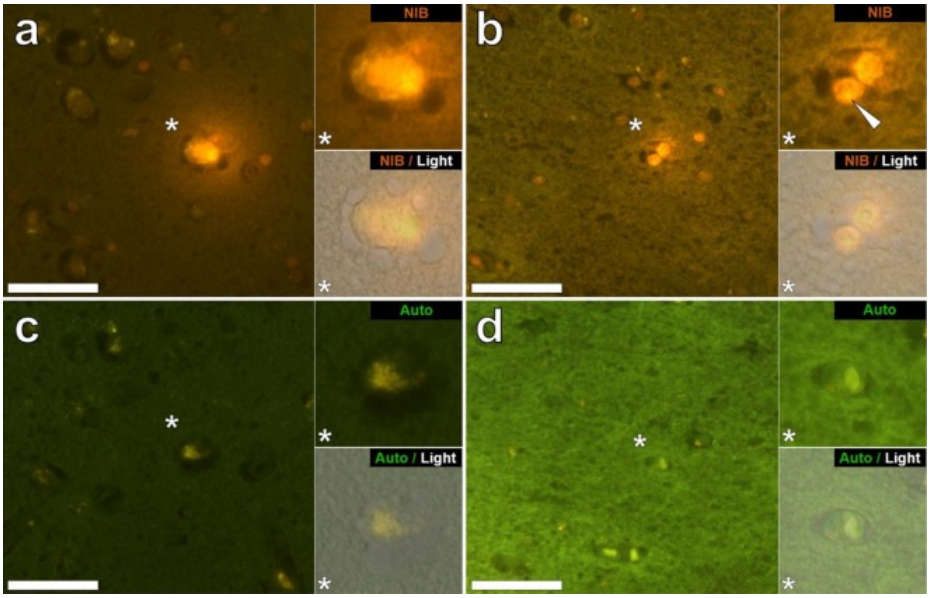

Download high-res image (708KB) Download full-size image

Fig. 5. Lumogallion-reactive aluminium in likely neuronal and glial cells in the temporal lobe and hippocampus of a 14-year-old male donor (A10), diagnosed with autism. Intraneuronal aluminium in the temporal lobe **(a)** was identified via an orange fluorescence emission, co-deposited with lipofuscin as revealed by a yellow fluorescence in the non-stained autofluorescence serial (5 μm) section **(c)**. Intracellular punctate orange fluorescence (white arrow) was observed in glia in the hippocampus **(b)** producing a green autofluorescence emission on the non-stained section **(d)**. Upper and lower panels depict magnified inserts marked by asterisks, of the fluorescence channel and bright field overlay. Magnification ×400, scale bars: 50 μm. (For interpretation of the references to colour in this figure legend, the reader is referred to the web version of this article.)

4. Discussion

The aluminium content of brain tissues from donors with a diagnosis of ASD was extremely high (Table 1). While there was significant inter-tissue, inter-lobe and inter-subject variability the mean aluminium content for each lobe across all 5 individuals was towards the higher end of all previous (historical) measurements of brain aluminium content, including iatrogenic disorders such as dialysis encephalopathy [13], [15], [16], [17], [18], [19]. All 4 male donors had significantly higher concentrations of brain aluminium than the single female donor. We recorded some of the highest values for brain aluminium content ever measured in healthy or diseased tissues in these male ASD donors including values of 17.10, 18.57 and 22.11 μg/g dry wt. (Table 1). What discriminates these data from other analyses of brain aluminium in other diseases is the age of the ASD donors. Why, for example would a 15 year old boy have such a high content of aluminium in their brain tissues? There are no comparative data in the scientific literature, the closest being similarly high data for a 42 year old male with familial Alzheimer's disease (fAD) [19].

Aluminium-selective fluorescence microscopy has provided indications as to the location of aluminium in these ASD brain tissues (Fig. 1, Fig. 2, Fig. 3, Fig. 4, Fig. 5). Aluminium was found in both white and grey matter and in both extra- and intracellular locations. The latter were particularly pre-eminent in these ASD tissues. Cells that morphologically appeared non-neuronal and heavily loaded with aluminium were identified associated with the meninges (Fig. 1), the vasculature (Fig. 2) and within grey and white matter (Fig. 3, Fig. 4, Fig. 5). Some of these cells appeared to be glial (probably astrocytic) whilst others had elongated nuclei giving the appearance of microglia [5]. The latter were sometimes seen in the environment of extracellular aluminium deposition. This implies that aluminium somehow had crossed the blood-brain barrier and was taken up by a native cell namely the microglial cell. Interestingly, the presence of occasional aluminium-laden inflammatory cells in the vasculature and the leptomeninges opens the possibility of a separate mode of entry of aluminium into the brain i.e. intracellularly. However, to allow this second scenario to be of significance one would expect some type of intracerebral insult to occur to allow egress of lymphocytes and monocytes from the vasculature [20]. The identification herein of non-neuronal cells including inflammatory cells, glial cells and microglia loaded with aluminium is a standout observation for ASD. For example, the majority of aluminium deposits identified in brain tissue in fAD were extracellular and nearly always associated with grey matter [19]. Aluminium is cytotoxic [21] and its association herein with inflammatory cells in the vasculature, meninges and central nervous system is unlikely to be benign. Microglia heavily loaded with aluminium while potentially remaining viable, at least for some time, will inevitably be compromised and dysfunctional microglia are thought to be involved in the aetiology of ASD [22], for example in disrupting synaptic pruning [23]. In addition the suggestion from the data herein

that aluminium entry into the brain via immune cells circulating in the blood and lymph is expedited in ASD might begin to explain the earlier posed question of why there was so much aluminium in the brain of a 15 year old boy with an ASD.

A limitation of our study is the small number of cases that were available to study and the limited availability of tissue. Regarding the latter, having access to only 1 g of frozen tissue and just 3 serial sections of fixed tissue per lobe would normally be perceived as a significant limitation. Certainly if we had not identified any significant deposits of aluminium in such a small (the average brain weighs between 1500 and 2000 g) sample of brain tissue then such a finding would be equivocal. However, the fact that we found aluminium in every sample of brain tissue, frozen or fixed, does suggest very strongly that individuals with a diagnosis of ASD have extraordinarily high levels of aluminium in their brain tissue and that this aluminium is pre-eminently associated with non-neuronal cells including microglia and other inflammatory monocytes.

5. Conclusions

We have made the first measurements of aluminium in brain tissue in ASD and we have shown that the brain aluminium content is extraordinarily high. We have identified aluminium in brain tissue as both extracellular and intracellular with the latter involving both neurones and non-neuronal cells. The presence of aluminium in inflammatory cells in the meninges, vasculature, grey and white matter is a standout observation and could implicate aluminium in the aetiology of ASD.

Competing interests

The authors declare that they have no competing interests.

Author contributions

CE designed the study, carried out tissue digests and TH GFAAS. DU carried out tissue digests and TH GFAAS. AK carried out brain neuropathology on sections prepared by MM. MM carried out all microscopy and with CE wrote the manuscript. All authors read and approved the manuscript.

Acknowledgements

The research is supported by a grant from the Children's Medical Safety Research Institute (CMSRI), a not-for-profit research foundation based in Washington DC, USA.

Appendix A. Supplementary data

The following are Supplementary data to this article:

Download Acrobat PDF file (244KB) Help with pdf files

Download Word document (15KB) Help with docx files

Recommended articles Citing articles (3)

References

[1] A. Krishnan, R. Zhang, V. Yao, C.L. Theesfeld, A.K. Wong, et al.
Genome-wide prediction and functional characterisation of the genetic basis of autism spectrum disorder
Nat. Neurosci., 19 (2016), pp. 1454-1462
CrossRef View Record in Scopus

[2] L.A. Sealey, B.W. Hughes, A.N. Sriskanda, J.R. Guest, A.D. Gibson, et al.
Environmental factors in the development of autism spectrum disorders
Environ. Int., 88 (2016), pp. 288-298
Article Download PDF View Record in Scopus

[3] R. Koyama, Y. Ikegaya
Microglia in the pathogenesis of autism spectrum disorders
Neurosci. Res., 100 (2015), pp. 1-5
Article Download PDF View Record in Scopus

[4] Q. Li, J.-M. Zhou
The microbiota-gut-brain axis and its potential therapeutic role in autism spectrum disorder
Neuroscience, 324 (2016), pp. 131-139
Article Download PDF View Record in Scopus

[5] C. Kaur, G. Rathnasamy, E.-A. Ling
Biology of microglia in the developing brain
J. Neuropathol Exp. Neurol., 76 (2017), pp. 736-753
View Record in Scopus

[6] M. Varghese, N. Keshav, S. Jacot-Descombes, T. Warda, B. Wicinski, et al.
Autism spectrum disorder: neuropathology and animal models
Acta Neuropathol., 134 (2017), pp. 537-566
CrossRef View Record in Scopus

[7] H. Yasuda, Y. Yasuda, T. Tsutsui
Estimation of autistic children by metallomics analysis
Sci. Rep., 3 (2013), p. 1199

[8] F.E.B. Mohamed, E.A. Zaky, A.B. El-Sayed, R.M. Elhossieny, S.S. Zahra, et al.
Assessment of hair aluminium, lead and mercury in a sample of autistic Egyptian children: environmental risk factors of heavy metals in autism
Behav. Neurol. (2015), p. 545674
(Art)

[9] M.H. Rahbar, M. Samms-Vaughn, M.R. Pitcher, J. Bressler, M. Hessabi, et al.
Role of metabolic genes in blood aluminium concentrations of Jamaican children with and without autism spectrum disorder
Int. J. Environ. Res. Public Health, 13 (2016), p. 1095
CrossRef

[10] A.V. Skalny, N.V. Simashkova, T.P. Klyushnik, A.R. Grabeklis, I.V. Radysh, et al.
Analysis of hair trace elements in children with autism spectrum disorders and communication disorders
Trace Elem. Med. Biol., 177 (2017), pp. 215-223
CrossRef View Record in Scopus

[11] L. Tomljenovic, C.A. Shaw
Do aluminium vaccine adjuvants contribute to the rising prevalence of autism?
J. Inorg. Biochem., 105 (2011), pp. 1489-1499
Article Download PDF View Record in Scopus

[12] C.A. Shaw, Y. Li, L. Tomljenovic
Administration of aluminium to neonatal mice in vaccine-relevant amounts is associated with adverse long term neurological outcomes
J. Inorg. Biochem., 128 (2013), pp. 237-244
Article Download PDF View Record in Scopus

[13] E. House, M. Esiri, G. Forster, P. Ince, C. Exley
Aluminium, iron and copper in human brain tissues donated to the medical research council's cognitive function and ageing study
Metallomics, 4 (2012), pp. 56-65
CrossRef View Record in Scopus

[14] M. Mold, H. Eriksson, P. Siesjö, A. Darabi, E. Shardlow, C. Exley
Unequivocal identification of intracellular aluminium adjuvant in a monocytic THP-1 cell line
Sci. Rep., 4 (2014), p. 6287

[15] A. Mirza, A. King, C. Troakes, C. Exley
The identification of aluminium in human brain tissue using lumogallion and fluorescence microscopy
J. Alzh. Dis., 54 (2016), pp. 1333-1338
CrossRef View Record in Scopus

[16] C. Exley, M. Esiri
Severe cerebral congophilic angiopathy coincident with increased brain aluminium in a resident of Camelford, Cornwall UK

J. Neurol. Neurosurg. Psychiatry, 77 (2006), pp. 877-879
CrossRef View Record in Scopus

[17] C. Exley, E.R. House
Aluminium in the human brain
Monatsh. Chem., 142 (2011), pp. 357-363
CrossRef View Record in Scopus

[18] C. Exley, T. Vickers
Elevated brain aluminium and early onset Alzheimer's disease in an individual occupationally exposed to aluminium: a case report
J. Med. Case Rep., 8 (2014), p. 41

[19] A. Mirza, A. King, C. Troakes, C. Exley
Aluminium in brain tissue in familial Alzheimer's disease
J. Trace Elem. Med. Biol., 40 (2017), pp. 30-36
Article Download PDF View Record in Scopus

[20] R. Shechter, O. Miller, G. Yovel, N. Rosenzweig, A. London, et al.
Recruitment of beneficial M2 macrophages to injured spinal cord is orchestrated by remote brain choroid plexus
Immunity (38 2013), pp. 555-569
Article Download PDF View Record in Scopus

[21] C. Exley
The toxicity of aluminium in humans
Morphologie, 100 (2016), pp. 51-55
Article Download PDF View Record in Scopus

[22] M.W. Salter, B. Stevens
Microglia emerge as central players in brain disease
Nat. Med., 23 (2017), pp. 1018-1027
CrossRef View Record in Scopus

[23] U. Neniskyte, C.T. Gross
Errant gardeners: glial-cell-dependent synaptic pruning and neurodevelopmental disorders
Nat. Rev. Neurosci., 18 (2017), pp. 658-670
CrossRef View Record in Scopus

© 2017 The Authors. Published by Elsevier GmbH.

ELSEVIER About ScienceDirect Remote access Shopping cart Contact and support Terms and conditions Privacy policy

Cookies are used by this site. For more information, visit the cookies page.
Copyright © 2018 Elsevier B.V. or its licensors or contributors. ScienceDirect ® is a registered trademark of Elsevier B.V.

RELX Group™